

BOILING HEAT TRANSFER MEASUREMENTS ON HIGHLY CONDUCTIVE SURFACES USING MICROSCALE HEATER AND TEMPERATURE ARRAYS

J. Kim¹, S.W. Bac², M.W. Whitten¹, J.D. Mullen¹, R.W. Quine¹, and T.S. Kalkur³

¹University of Denver, Department of Engineering, Denver, CO 80208, jkim@du.edu, ²Pohang University of Science and Technology, Department of Mechanical Engineering, Pohang, Kyungbuk, 790-784, Korea, bswon@postech.ac.kr, ³University of Colorado, Department of Electrical Engineering, Colorado Springs, CO 80933, kalkur@vlsie.uccs.edu.

ABSTRACT

Two systems have been developed to study boiling heat transfer on the microscale. The first system utilizes a 32 x 32 array of diodes to measure the local temperature fluctuations during boiling on a silicon wafer heated from below. The second system utilizes an array of 96 microscale heaters each maintained at constant surface temperature using electronic feedback loops. The power required to keep each heater at constant temperature is measured, enabling the local heat transfer coefficient to be determined. Both of these systems as well as some preliminary results are discussed.

INTRODUCTION

The vast majority of experimental work performed to date regarding boiling has utilized single heaters that were large compared to individual bubble sizes, making it difficult to look at details of the boiling process. These experiments usually used a heating element operated in a constant heat flux mode, making it difficult to study transition boiling effects beyond critical heat flux (CHF). Other experiments have utilized surfaces held at constant temperature, but the *local* heat flux and temperature were not measurable and can vary significantly across the heater. Even when local measurements were obtained (e.g., Cooper and Lloyd--1969, Hohl, et al.--1997), this was done at only a few locations on the heater surface. The pioneering work of Kenning (1992) and Watwe and Hollingsworth (1994) using liquid crystals on thin, electrically heated stainless steel plates did much to elucidate the heat transfer mechanisms associated with large scale phenomenon because information regarding temperature fluctuations were available with high resolution across the heater surface. The work described in this paper complements the liquid crystal work in that boiling on a comparatively small heated area is investigated in detail with high spatial and temporal resolution.

It must be remembered that boiling behavior on small heated areas can differ from that on large heated areas. First, the total number of nucleation sites is much smaller, and can result in heaters smaller than the corresponding average distance between nucleation sites on large heaters. Boiling can be delayed to higher wall superheats as a result, or the number of

nucleation sites may not be statistically representative. Second, the Taylor wavelength, which is significant at CHF and transition and film boiling, can be larger than the heater size. Third, edge-effects can become significant.

DIODE ARRAY

This technique uses a 32 x 32 array of silicon diodes constructed on a silicon substrate to obtain the surface temperature distribution by measuring the forward voltage drop across each diode. Silicon diodes typically have a forward voltage drop of 0.7 V that decreases by 2 mV for every 1 °C increase in temperature near room temperature. The voltage drop across a diode is approximately proportional to the inverse of the absolute temperature of the diode for a wide range of temperatures.

Use of silicon diodes to measure temperature is not new. Diodes and the associated electronics specifically designed to measure temperature are commercially available (two suppliers are Validyne Engineering and Lake Shore Cryotronics). The main application of silicon diode temperature sensors is in measuring cryogenic temperatures since the forward voltage drop changes rapidly with temperature at low temperatures, although commercially available units cite useful temperature ranges from 1.4 K to 475 K.

The advantages of using a diode array to measure temperature rather than microthermocouples or liquid crystals are that 1). the temperature can be measured at many more points than is possible using microthermocouples, 2). temperature fluctuations over a much wider range can be measured compared to liquid crystals, 3). the resolution of the temperature measurements is much better than is possible using liquid crystals. The main limitation on the current technique is that the measurements are confined to relatively small areas.

The ultimate goal of this work is to determine local heat transfer coefficients by measuring the local temperatures vs. time, then numerically determining the local heat flux. One difficulty with using a silicon substrate is that the high thermal conductivity of silicon tends to smear out temperature gradients, making the determination of local heat flux difficult. An option is to build the diode array on a 0.2 μm layer of single crystal silicon-on-quartz substrate. Because quartz has a much lower thermal conductivity than silicon ($k_{Si}=135$ W/m-K, $k_{Qtz}=1.5$ W/m-K), small

changes in heat transfer from the surface result in relatively large changes in temperature, greatly increasing the accuracy of the numerically determined heat flux. This technology has the added advantage that the silicon layer is transparent, allowing visual observations from beneath the heater to be made while measuring heat flux distributions. Work is currently progressing on building such a diode array.

In the current configuration, a chip containing the diodes is heated from below using a cartridge heater embedded in an aluminum rod. Thermocouples along the rod measure the temperature gradient along the rod enabling the heat flux to be determined.

Description of the diode array. An example of how the diodes would be connected together is shown on Figure 1 for a 3 x 3 array of diodes. If the voltage drop across diode A-2 is desired, a current (typically 1 mA) is sent into row A while the other rows are grounded. Simultaneously, column 2 is grounded while the other columns are set to 5 V. All of the diodes in the array with the exception of A-2 are now either reverse biased or have no voltage drop across them. The voltage at A is then measured to obtain the forward voltage drop across diode A-2. The voltage drop across the other diodes in the array are obtained by scanning across the array. A 32 x 32 p-n junction isolated diode array was built on a p-type wafer using VLSI techniques—a photograph of a diode in the array is shown on Figure 2.

Up to eight arrays can be made on a single wafer. Once a wafer has been processed, the wafer is diced to obtain the individual chips. These chips are epoxied to a Pin Grid Array (PGA), and connections from the chips to the PGA are made using wire-bonds.

The current used to sense the voltage drop across the diode must not influence the temperature measurement by heating the diode significantly. The energy dissipated by a typical diode with a 1 mA sensing current is 7 W/cm². While this may seem like a large heat flux, it must be remembered that the sensing current is only applied for a very short time (typically 1 μs if scanning occurs at 1 MHz for a 32 x 32 array). An upper bound on the temperature rise of the surface can be obtained by assuming that the silicon substrate acts as a semi-infinite solid subjected to a step change in wall heat flux (Incropera and Dewitt—1996):

$$T(0, t) - T_i = \frac{2q_0(\alpha t / \pi)^{1/2}}{k}$$

For the conditions described above, the surface temperature rise is just 0.005 °C, which is well within the uncertainty of the measurement. The actual temperature rise is much lower since only a small portion of the surface is heated.

Description of circuitry and data acquisition unit. An electronic circuit is used to scan the diodes in the array and provide signal conditioning. The circuit receives two external signals: a start pulse and a signal from an external clock, both of which enter a counter. The start pulse tells the counter to begin counting, while the external clock is used to set the frequency at which counting occurs. The actual counting frequency is half the clock frequency. Counting frequencies of up to 2.5 MHz are possible with the current circuitry. The signal exiting the counter enters two Erasable Programmable Read Only Memories (EPROM), one for choosing the row and one for choosing the column. Every time a pulse from the clock enters the EPROMs, they output two 5-bit digital signals corresponding to row and column numbers. In the present configuration, all of the diodes in a particular row are scanned before going on to the next row. The entire array is scanned once every time the circuit receives an external start pulse.

The measured voltage drops across the diodes are multiplexed into one continuous signal that is typically between 0.8–0.6 V. To take advantage of the resolution of the A/D converter (12 bit, 0-5V), this signal is sent through a signal conditioning unit that offsets, inverts, and amplifies the signal to match a 0-5 V range.

Calculations indicate that the A/D converter should be able to resolve temperature changes in the diodes as small as 0.05 °C. This is based on 12 bits of resolution, an assumed range in voltage drop of 0.8-0.6 V, and the measured change in voltage drop with temperature.

Calibration. Calibration of the diode array is performed by placing the array in an oil bath at known temperature and measuring the voltage output from the circuit vs. the bath temperature. An accurate value of the thermal conductivity of the aluminum rod is needed in order to compute the heat flux through the silicon. A bar of aluminum from the same stock used to heat the chip was machined so that it could be heated from one end using the same type of cartridge heater used to heat the chip. Thermocouples along the rod were used to measure the temperature gradient along the rod. Numerical simulation of the temperatures in the rod and surrounding insulation showed that the heat transfer through the insulation was negligible compared to the heat transferred along the rod. The thermal conductivity of the aluminum was computed from the data to be 243 W/m-K.

Preliminary results. The concept was tested on a 3 x 3 array of commercially available diodes connected to the circuit. The output was observed on an oscilloscope as each diode was heated in turn using a hot-air gun. As expected, the output voltage from the circuit was observed to increase with increasing temperature.

Once the concept was verified, a 32 x 32 diode array was constructed. It was found, however, that the interconnects between diodes in the vertical direction were faulty. Only half of the bottom row of diodes (a total of 16 diodes) could therefore be addressed. The problem with the interconnects is currently being fixed, and a new diode array is being constructed.

Calibration of the 16 working diodes in the current array was performed—a plot of voltage drop vs. temperature for these diodes is shown on Figure 3. The change in voltage drop across the diodes is nominally $-1.1 \text{ mV}/^\circ\text{C}$. The difference between the measured value and the ideal value of $-2 \text{ mV}/^\circ\text{C}$ is thought to be due to the use of a recycled silicon wafer. The new diode array is being built on a prime grade wafer.

CONSTANT TEMPERATURE HEATER ARRAY

The local wall heat flux variations in boiling of FC-72 on a small heated area was examined using an array of microscale heaters each maintained at constant surface temperature. The scale of the individual heaters was approximately the same as that of the departing bubbles in nucleate boiling. The information contained in this paper is unique in that data was taken at many points simultaneously instead of at a single point, enabling a much more detailed picture of the heat transfer process to be obtained. An additional advantage of this work is that the heat flux was measured directly, instead of being inferred from average heat flux data and void fraction measurements.

Experimental apparatus. Much of the experimental apparatus has been discussed elsewhere (Rule, et al.—1997, Rule and Kim—1997, Rule—1998), so only a brief summary of the experimental apparatus will be given here. Local surface heat flux and temperature measurements are provided by an array of platinum resistance heater elements deposited on a quartz wafer in a serpentine pattern. Each of these elements is $0.26 \text{ mm} \times 0.26 \text{ mm}$ in size, and have a nominal resistance of $1000 \ \Omega$ and a nominal temperature coefficient of resistance of $0.002 \ ^\circ\text{C}^{-1}$. Ninety six individual heaters are arranged in a square array about 2.7 mm on a side, as shown in Figure 4.

The temperature of each heater in the array is kept constant by a feedback circuit similar to that used in constant temperature hot-wire anemometry (Figure 5). The control resistor in the circuit is a digital potentiometer from Dallas Semiconductor. The instantaneous power required to keep each heater at a constant temperature is measured and used to determine the heat flux from each heater element. Because all the heaters in the array are at the same temperature, heat conduction between adjacent heaters is negligible. There is conduction from each heater

element to the surrounding quartz substrate, but this can be measured and subtracted from the total power supplied to the heater element, enabling the power supplied to the fluid to be determined.

Shown on Figure 6 is a schematic of an experimental apparatus provided by NASA and used in these studies. The bellows and the surrounding housing allowed the test section pressure to be controlled. A stirrer was used to break up stratification within the test chamber, while a temperature controller and a series of Kapton heaters attached to the boiling chamber were used to control the bulk fluid temperature. The fluid was degassed by pulling a vacuum on the fluid. The final dissolved gas concentration in the liquid, determined using the chamber temperature and pressure and the properties of FC-72 (3M Fluorinert Manual--1995), was less than 1.5×10^{-3} moles/mole.

Heater calibration. The heater array was calibrated in an insulated, circulating constant temperature oil bath which was held within $0.2 \ ^\circ\text{C}$ of the calibration temperature. An impinging jet of oil onto the heater provided a high heat transfer coefficient. Calibration consisted of finding the value of the control resistor (R_{control} in Figure 5) that causes the feedback loop to just begin regulating.

Results from previous work. Detailed results of saturated, pool boiling of FC-72 with this heater facing upward were presented in Rule and Kim (1997) and Rule (1998). The results presented include spatially-averaged time-averaged data, spatially-averaged time-resolved data, time-resolved data from individual heaters in the array, as well as spatially-resolved time-averaged data. Other results included data that was conditionally sampled on boiling, as well as the heat flux during liquid contact in the transition boiling regime. Some of the main conclusions resulting from this work were:

- 1). The inner heaters reach CHF at lower wall superheats than that for the array averaged heat flux.
- 2). Significant variations in boiling fraction occur over the surface of small heaters during nucleate and transition boiling, indicating that point measurements of heat flux, temperature, or void fraction may not be representative of average boiling behavior.
- 3). Vapor patches at CHF and during transition boiling were observed to move with time, and were related to the bubble dynamics above the heater.
- 4). Heat transfer during liquid contact in transition boiling was constant for a given wall superheat for the inner heaters, and was observed to decrease with increasing wall superheat.

Recent results. Visualization of the bubble behavior on the surface along with heat transfer measurements has recently been performed. The semi-transparent nature of the heater array enabled high speed digital videos (SpeedCam, monochrome, 1000

fps, 512 x 512 resolution with an Infinity Optical KC microscope lens with IF-4 objective) to be made of the bubbles from below.

Some preliminary data taken under saturated, pool boiling conditions is discussed. A snapshot of boiling in the isolated bubble regime ($\Delta T_{\text{sat}}=29$ °C, $T_{\text{sat}}=51$ °C in Denver, CO) was shown on Figure 4. Heat flux data was obtained at 2500 Hz, while videos were taken at 1000 Hz with 512 x 512 resolution. Shown on Figure 7 is the time varying evolution of the bubble on the upper left corner of the heater array (the bubble growing on heaters 44 and 72-74). The corresponding heat flux traces on selected heaters is shown on Figure 8. Between 14 and 15 ms, the shadow from the bubble that departed previously is seen. Nucleation of a new bubble occurs between 16 ms and 18 ms—this corresponds to a sharp increase in the wall heat flux. The formation of what appears to be a dry spot underneath the growing bubble occurs soon after nucleation. This dry spot shrinks in size starting from 18 ms and seems to disappear around 21 ms, which corresponds to a sharp drop in wall heat transfer. The detached bubble moves away from the surface between 21 ms and 28 ms. It is interesting to note that there is a large amount of heat transfer associated with nucleation, but also a large amount of heat transfer as the dry spot shrinks and liquid re-wets the wall. The magnitude of heat transfer during re-wetting of the wall is smaller than during nucleation, but is of longer duration, resulting in comparable overall heat transfer rates. The heat transfer after bubble departure is very low in comparison.

The large heat transfer associated with nucleation could be due to evaporation of the microlayer, as postulated. The numerical models, however, do not seem to predict the large amounts of heat that are transferred just before the bubble departs the surface. The heat transfer mechanism seen is different from the widely accepted view that microlayer evaporation is the dominant heat transfer mechanism in saturated pool boiling. It is important to note that this data is preliminary—data from other bubbles on the surface suggest different heat transfer mechanisms.

CONCLUSIONS

Two techniques for making local measurements in boiling heat transfer have been developed. One technique measures wall temperature on a wall with constant heat flux, while the other measures wall heat flux on a wall held at constant temperature. Both methods promise to help clarify boiling heat transfer mechanisms.

ACKNOWLEDGEMENTS

The funding for this work was provided by NASA MSAD, and is gratefully acknowledged. The grant monitor is Mr. John McQuillen.

REFERENCES

- 3M Corporation, 1995, *3M Fluorinert Liquids Product and Contact Guide*.
- Cooper, M.G. and Lloyd, A.J.P., 1969, "The microlayer in nucleate boiling", *International Journal of Heat and Mass Transfer*, Vol. 12, pp. 895-913.
- Hohl, R., Auracher, H., Blum, J., and Marquardt, W. (1997), "Identification of Liquid-Vapor Fluctuations Between Nucleate and Film Boiling in Natural Convection", Proceedings of the 1997 Engineering Foundation Conference on Convective Flow and Pool Boiling, Irsee, Germany.
- Incropera, F.P. and Dewitt, D.P., 1996, *Fundamentals of Heat and Mass Transfer*, Fourth Edition, John Wiley and Sons.
- Kenning, D.B.R., 1992, "Wall Temperature Patterns in Nucleate Boiling", *International Journal of Heat and Mass Transfer*, Vol. 35, pp. 73-86.
- Rule, T.D., Kim, J., Quine, R.W., Kalkur, T.S., and Chung, J.N., 1997, "Measurements of Spatially and Temporally Resolved Heat Transfer Coefficients in Subcooled Pool Boiling", Proceedings of the 1997 Engineering Foundation Conference on Convective Flow and Pool Boiling, Irsee, Germany.
- Rule, T.D. and Kim, J., 1997, "Wall Heat Transfer Measurements in Saturated Pool Boiling of FC-72 on a Small Heated Area", proceedings of the ASME IMECE conference, Dallas, TX.
- Rule, T.D., 1998, "Design, Construction and Qualification of a Microscale Heater Array for Use in Boiling Heat Transfer", Master's Thesis, School of Mechanical and Materials Engineering, Washington State University, Pullman, WA.
- Watwe, A.A. and Hollingsworth, D.K., 1994, "Liquid Crystal Images of Surface Temperature During Incipient Pool Boiling", *Experimental Thermal and Fluid Science*, Vol. 9, pp. 22-33.

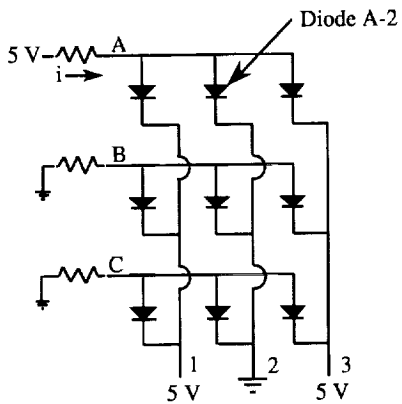


Figure 1: Example of a 3 x 3 diode array.

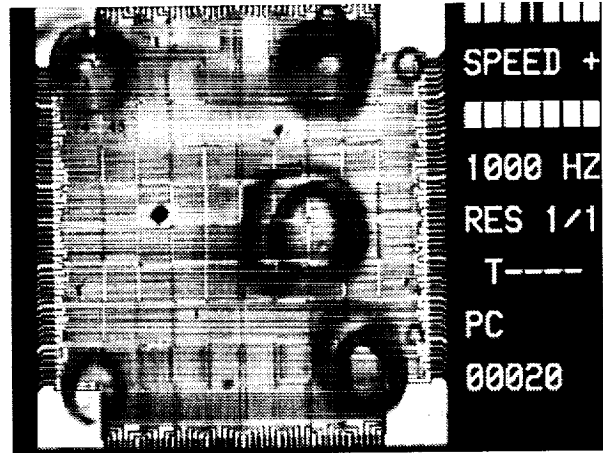


Figure 4: Photograph of boiling on the heater array— isolated bubble regime. Each heater in the array is 0.27 mm x 0.27 mm in size.

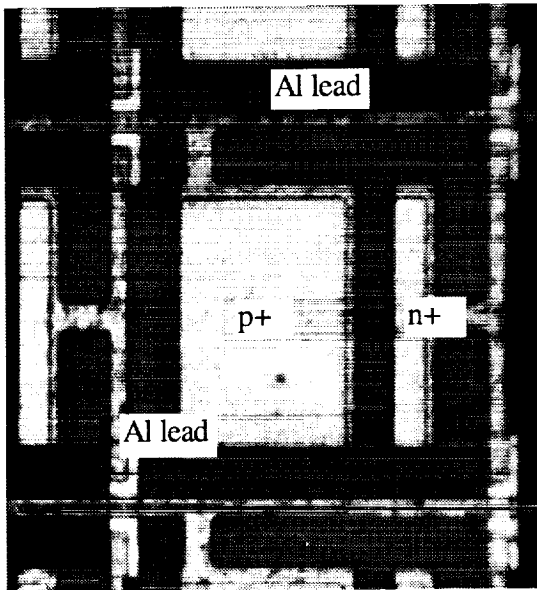


Figure 2: Photograph of a diode in the array.

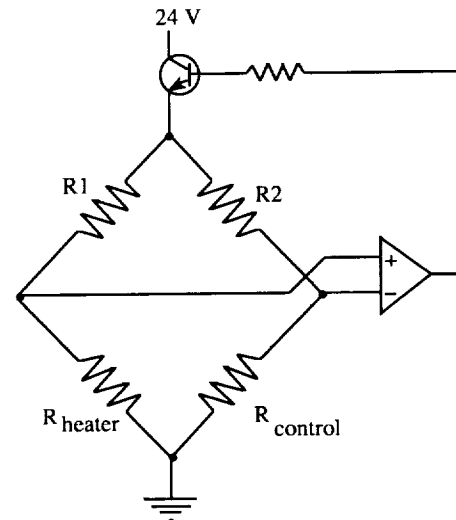


Figure 5: Schematic of feedback loop.

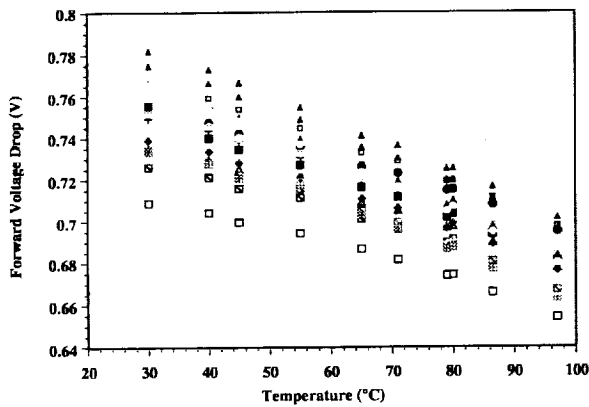


Figure 3: Calibration of diode array.

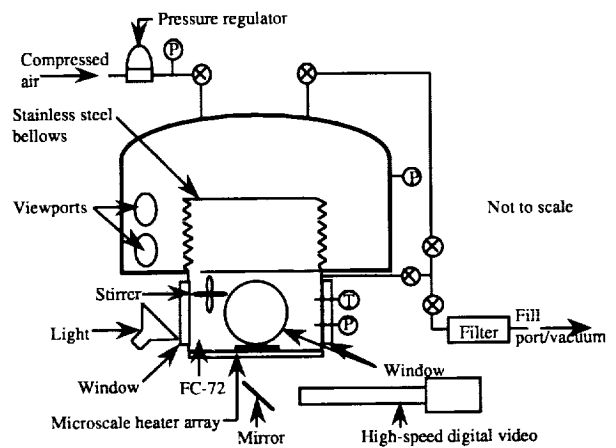


Figure 6: Schematic of experimental apparatus.

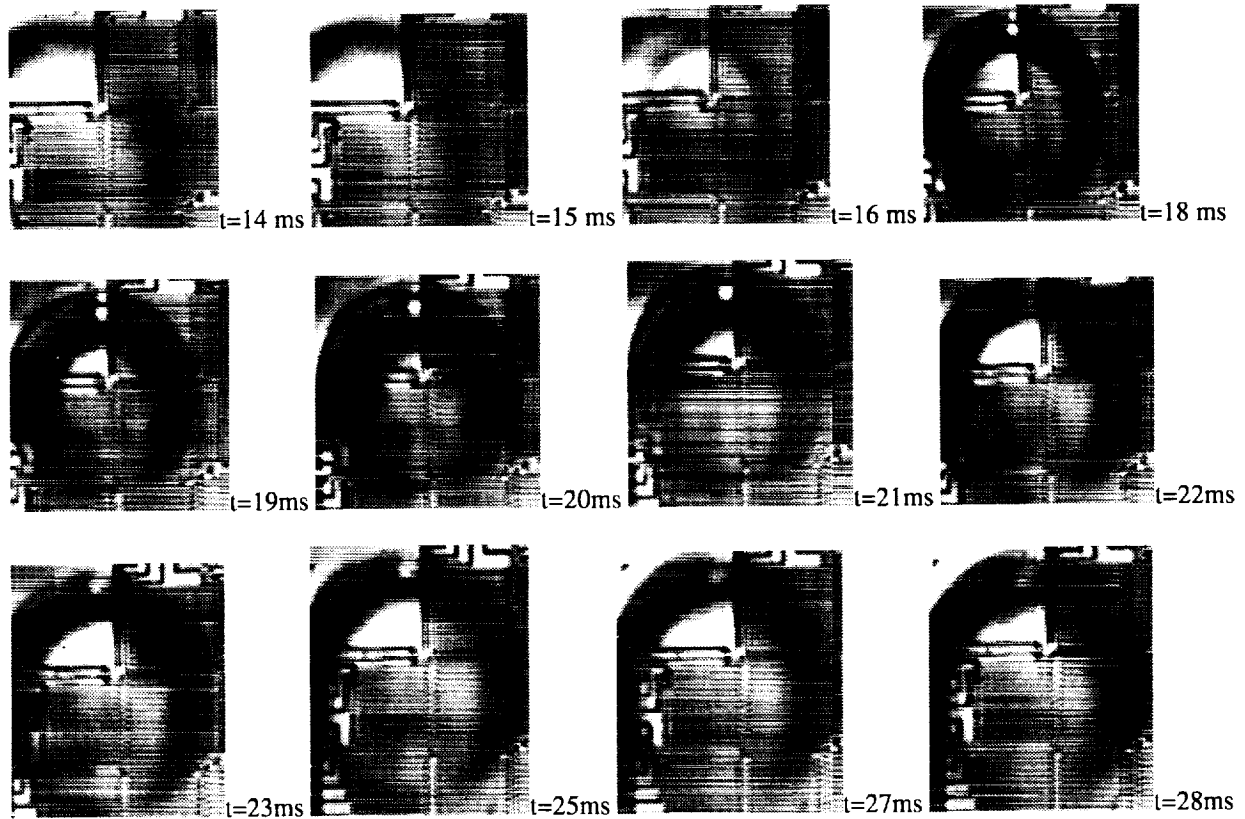


Figure 7: Evolution of one bubble on the surface.

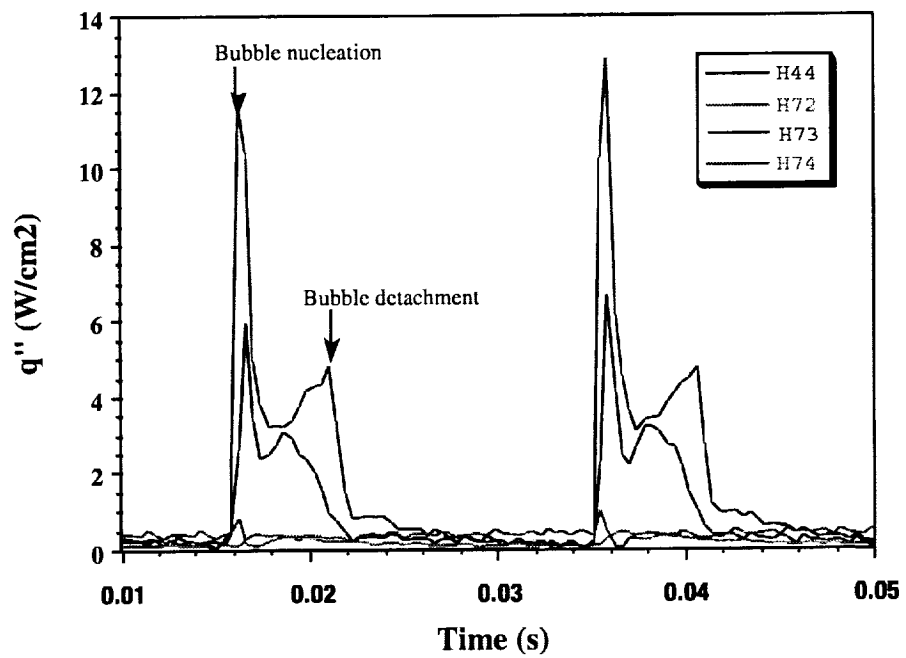


Figure 8: Wall heat flux vs. time for selected heaters. The times correspond to those on Figure 7.